



HAL
open science

Unbiased evaluation of zero-field splitting D parameter in high-spin molecules from DC magnetic data with incomplete powder averaging

Andrea Cornia, Anne-Laure Barra, Giordano Poneti, Erik Tancini, Roberta Sessoli

► **To cite this version:**

Andrea Cornia, Anne-Laure Barra, Giordano Poneti, Erik Tancini, Roberta Sessoli. Unbiased evaluation of zero-field splitting D parameter in high-spin molecules from DC magnetic data with incomplete powder averaging. *Journal of Magnetism and Magnetic Materials*, 2020, 510, pp.166713. 10.1016/j.jmmm.2020.166713 . hal-02912243

HAL Id: hal-02912243

<https://hal.science/hal-02912243>

Submitted on 17 Jul 2023

HAL is a multi-disciplinary open access archive for the deposit and dissemination of scientific research documents, whether they are published or not. The documents may come from teaching and research institutions in France or abroad, or from public or private research centers.

L'archive ouverte pluridisciplinaire **HAL**, est destinée au dépôt et à la diffusion de documents scientifiques de niveau recherche, publiés ou non, émanant des établissements d'enseignement et de recherche français ou étrangers, des laboratoires publics ou privés.

Unbiased evaluation of zero-field splitting D parameter in high-spin molecules from DC magnetic data with incomplete powder averaging

Andrea Cornia^{a,*}, Anne-Laure Barra^b, Giordano Poneti^c, Erik Tancini^a, Roberta Sessoli^d

^a*Department of Chemical and Geological Sciences, University of Modena and Reggio Emilia & INSTM, 41125 Modena, Italy*

^b*Laboratoire National des Champs Magnétiques Intenses-CNRS, Université Grenoble-Alpes, 38042 Grenoble Cedex 9, France*

^c*Instituto de Química, Universidade Federal do Rio de Janeiro, Rio de Janeiro, 21941-909 Brazil*

^d*Department of Chemistry ‘Ugo Schiff’, University of Florence & INSTM, 50019 Sesto Fiorentino (FI), Italy*

Abstract. A simple scheme is presented to account for preferential orientation effects in the DC magnetic response of polycrystalline samples of anisotropic high-spin molecules, like single-molecule magnets. A single additional least-squares parameter is introduced in the fitting of isothermal magnetization vs. field data to describe the leading part of a non-spherical distribution of anisotropy axes. The procedure is shown to afford an accurate D parameter and is potentially applicable whenever complete powder averaging cannot be achieved.

Keywords: single-molecule magnets – high-spin molecules – magnetic anisotropy – zero-field splitting – DC magnetometry – preferential orientation

*Corresponding author

E-mail address: acornia@unimore.it (A. Cornia)

1. Introduction

The analysis of magnetic data in molecular species has experienced a renaissance in the early 1990s, after the discovery that magnetic relaxation in molecules may dramatically slow down at low temperature, yielding magnetic bistability [1,2]. Research on such single-molecule magnets (SMMs) has advanced considerably in the last few years and some dysprosocenium derivatives engendered with a huge easy-axis magnetic anisotropy were found to display a memory effect above liquid nitrogen temperature [3–5]. This remarkable result shows that molecular materials have a real potential for magnetic storage application [6] and highlights the central role played by an accurate measurement and understanding of molecular anisotropy [7].

In mono- or polynuclear SMMs with quenched first-order orbital momentum and a well-isolated ground spin state, an especially widespread and standardized procedure is followed to retrieve the total spin value (S) and the leading, second-order axial anisotropy parameter (D) [8]. Working on polycrystalline samples, the value of S is customarily first estimated from the low-field low-temperature value of the χT product or from the saturation magnetization. It is then used in the analysis of M vs. H isotherms at low T based on zero-field splitting (zfs) *plus* Zeeman Hamiltonian:

$$\hat{H}_{zfs+Zee} = D[\hat{S}_z^2 - S(S + 1)/3] + \mu_B g \hat{\mathbf{S}} \cdot \mathbf{B} \quad (1)$$

where \mathbf{S} is the total spin vector, S_z is its component along the anisotropy axis (z) and an isotropic g -factor is assumed. *Ad-hoc* software, like the popular PHI program [9], allows to fit magnetic data to Eq. (1) as well as to include additional terms such as rhombic or higher-order anisotropies [8]. Calculated magnetization is obtained by orientational averaging [10–12] over a large number of sampling grid points, so as to simulate the response of a powder of randomly oriented crystallites. Experimentally, attaining a good “powder average” requires thorough grinding, followed by pelletization or immersion in wax (e.g. eicosane). These mechanical restraints are essential to avoid in-field orientation of crystallites due to strong magnetocrystalline anisotropy [3–5]. In certain circumstances, e.g. when only a minute sample amount is available, such a procedure may be difficult to carry out to the desired level of accuracy. More fundamentally, deep grinding of very reactive samples may greatly facilitate their reaction with the environment. Samples containing volatile and weakly bound crystallization solvent may also suffer from such procedure, as it accelerates solvent loss and causes structural alterations which may significantly bias the magnetic properties of the pristine phase. The actual

distribution of crystallites in samples affected by incomplete powder averaging may be difficult to predict, although it is influenced by crystal morphology and structure.

We have encountered similar situations in our laboratories [13] and have developed a very simple correction scheme, based on a single parameter, that allows to extract the D value in Eq. (1) even in the presence of preferential orientation [14] and without significant bias. The only requirement is that the distribution of crystallites remains unchanged during the measurements, a condition certainly met in a properly restrained sample. Qualitatively similar, but more elaborated procedures are widely used in magnetic resonance techniques like EPR [15,16] and in powder diffraction [17]. We have tested the method on an SMM of the Fe_4 family, namely $[\text{Fe}_4(\text{L})_2(\text{dpm})_6]$ (**1**) where H_3L is tripodal proligand 5-(acetylthio)-2,2-bis(hydroxymethyl)pentan-1-ol and Hdpm is dipivaloylmethane [18]. The compounds of this class comprise four high-spin iron(III) ions ($s_i = 5/2$) arranged in a centered-triangular fashion and antiferromagnetically coupled to give a ground spin state with $S = 5$ (see Fig. 1, left inset). This ground manifold is well isolated from excited states, which lie 55-65 K higher in energy, and undergoes predominantly axial zfs with D ranging from -0.21 to -0.45 cm^{-1} in Eq. (1), depending on the specific structure. In complexes with two coordinated tripodal ligands, like **1**, D spans a much more limited range (from -0.40 to -0.45 cm^{-1}) [19]. The magnetic easy axis (z) is directed close to the normal to the Fe_4 plane, or exactly along it when molecules exhibit crystallographic threefold symmetry [20].

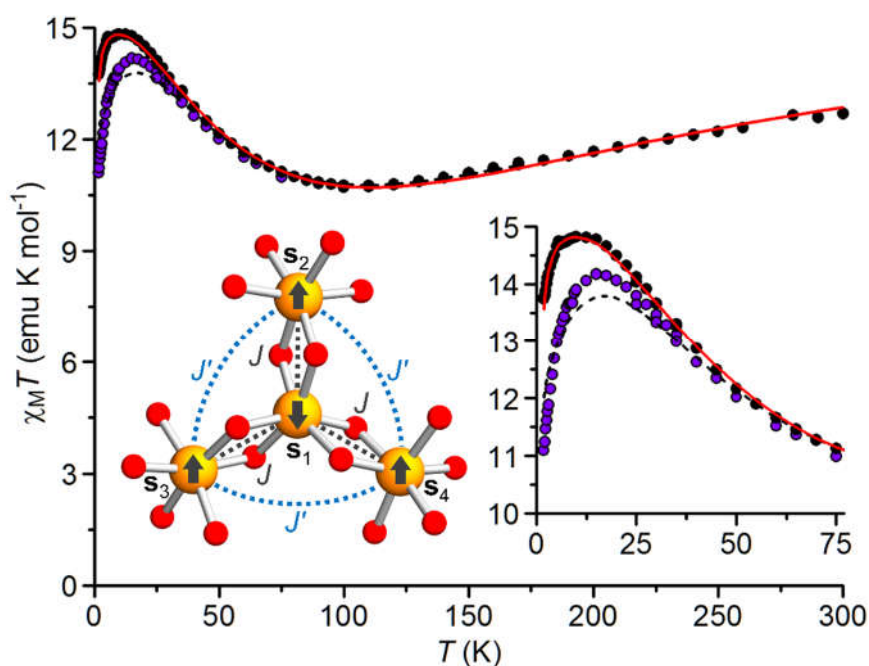


Fig. 1. Low-field $\chi_M T$ vs. T plot recorded on a vertically oriented pellet (see Fig. 2, inset) after rough crushing (violet circles) and thorough grinding (black circles) of the sample. The black dashed and red solid curves provide the best fit to the two datasets with g , J , J' and B_2^0 values reported in section 3. Insets: (left) Fe/O core of Fe_4 complexes (orange = Fe, red = O), with the definition of superexchange coupling constants (J , J'), and the arrangement of spin vectors (\mathbf{s}_i) in the ground $S = 5$ state; (right) enlarged view of the low- T region. (For interpretation of the references to color in this figure legend, the reader is referred to the web version of this article.)

2. Materials and methods

H_3L was obtained by Tollens condensation of 4-pentenal with formaldehyde and CaO in EtOH/ H_2O to give 2,2-bis(hydroxymethyl)-4-penten-1-ol, and subsequent radical addition of thioacetic acid to the terminal double bond, as reported for a longer-chain congener [21]. Compound **1** was prepared by reaction of excess H_3L with $[\text{Fe}_4(\text{OMe})_6(\text{dpm})_6]$ [20] in anhydrous Et_2O and recrystallized from anhydrous 1,2-dimethoxyethane [22]. Details on the synthesis and crystal structure of **1** are out of the scope of this paper and are left for a more specialized publication.

Crystals of the compound were roughly crushed and pressed into a pellet (20.38 mg, 3 mm in diameter), which was measured in vertical orientation on a SQUID magnetometer equipped with a 50-kOe magnet (Quantum Design MPMS). The same sample was remeasured in both vertical and horizontal orientations on a vibrating-sample magnetometer (VSM) working with fields up to 60 kOe (Quantum Design PPMS). The sample was then thoroughly grinded, pelletized (12.34 mg, 3 mm in diameter) and measured again in vertical orientation on SQUID magnetometer (pellet orientation is defined in the inset of Fig. 2). Magnetic susceptibility was obtained as M/H from magnetization (M) measurements at $T = 1.8\text{-}300$ K and $H = 10$ kOe (but 1 kOe at $T \leq 30$ K). M vs. H isotherms were recorded at three temperatures between 1.9 and 5.0 K in applied fields up to 50-60 kOe. Raw data were corrected for the contribution of sample holder and addenda, and converted to molar magnetic susceptibility (χ_M) and molar magnetization (M_M) using the appropriate molar mass ($1761.56 \text{ g mol}^{-1}$) and diamagnetic correction ($-1004.4 \cdot 10^{-6} \text{ emu mol}^{-1}$) [23].

The fitting of $\chi_M T$ vs. T curves was done with PHI program (v3.1.5) using a 144-point Zaremba-Conroy-Wolfsberg (ZCW) scheme for powder integration (FIELD POWDER 4) [9]. M_M vs. H curves were fitted using in-house developed software in FORTRAN language based on F02ABF and E04FCF NAG routines for matrix diagonalization and least-squares (LS) fitting, respectively [24]. The estimated standard deviation of each best-

fit parameter in Table 1 was calculated from the variance-covariance matrix, as provided by routine E04YCF [24].

HF-EPR powder spectra were recorded with a multifrequency spectrometer, operating in double-pass configuration at temperatures ranging from 5 to 20 K and in magnetic fields up to 12 T. The measurements were carried out at two frequencies, 190 GHz or 230 GHz, obtained from Gunn diode sources coupled to frequency doublers. They were performed on a pelletized sample to avoid field-induced orientation effects. The spectra were simulated using parameters obtained through the fitting of the resonance positions [25,26].

3. Results and discussion

In Fig. 1 and 2 we present the DC magnetic properties of a sample of **1** prepared by compressing roughly crushed crystals into a pellet. The pellet was oriented vertically in a SQUID magnetometer, so as to be probed in-plane by the magnetic field. The low-field molar susceptibility χ_M is shown in Fig. 1 as a $\chi_M T$ vs. T plot (violet circles). At ca. 15 K the curve approaches a maximum value of $14.3 \text{ emu K mol}^{-1}$, which is reasonably close to the Curie constant for a $S = 5$ state with $g = 2.00$ ($15.0 \text{ emu K mol}^{-1}$). Upon further cooling, the $\chi_M T$ product drastically decreases in a way which is difficult to reconcile with the nature of the material. In the explored temperature and field range, saturation effects and intermolecular interactions, which are of dipolar type, contribute negligibly to the measured curve [27]. It is therefore tempting to ascribe the low temperature drop entirely to zfs effects. A quantitative treatment of the $\chi_M T$ vs. T curve was then undertaken using the PHI program [9] based on Hamiltonian:

$$\hat{H} = J\hat{\mathbf{s}}_1 \cdot (\hat{\mathbf{s}}_2 + \hat{\mathbf{s}}_3 + \hat{\mathbf{s}}_4) + J'(\hat{\mathbf{s}}_2 \cdot \hat{\mathbf{s}}_3 + \hat{\mathbf{s}}_3 \cdot \hat{\mathbf{s}}_4 + \hat{\mathbf{s}}_2 \cdot \hat{\mathbf{s}}_4) + B_2^0 \sum_{i=1}^4 \hat{O}_{2,i}^0 + \mu_B g \hat{\mathbf{S}} \cdot \mathbf{B} \quad (2)$$

where $\hat{O}_{2,i}^0 = 3\hat{s}_{z,i}^2 - s_i(s_i + 1)$ and $s_{z,i}$ is the z -component of \mathbf{s}_i [28]. In the first two terms, J and J' are the nearest-neighbor and next-nearest-neighbor superexchange interactions depicted in Fig. 1 (left inset). The third term embeds magnetic anisotropy, which is attributed entirely to four identical single-ion contributions through a common B_2^0 parameter. Notice that projection formulae relate B_2^0 to the D value in the $S = 5$ state, according to the equation $D = (188/91)B_2^0$ [22]. Finally, in the Zeeman term, \mathbf{S} is the total spin vector and the same isotropic g factor is used at all metal sites.

A LS fitting procedure gave $g = 1.942(6)$, $J = 14.5(5) \text{ cm}^{-1}$, $J' = -1.0(2) \text{ cm}^{-1}$ and $B_2^0 = -0.84(9) \text{ cm}^{-1}$, but the fit is very inaccurate in the low- T portion of the curve (Fig. 1, right inset); more important, with such a large on-site anisotropy the $|D|$ value in the $S = 5$ state is unrealistically large ($\sim 1.7 \text{ cm}^{-1}$).

The fitting of isothermal molar magnetization (M_M) vs. H curves recorded below 5 K in fields up to 50 kOe is also problematic using Eq. (1) (Fig. 2, main panel). The best-fit D parameter so obtained is reported in entry **a** of Table 1 and is too large in magnitude for a Fe_4 complex [19]. These difficulties in the analysis of magnetic data arise because of incomplete powder averaging in the sample. The same pellet was transferred to a VSM and measured both in vertical and horizontal orientations, with fields up to 60 kOe applied in-plane and out-of-plane, respectively (Fig. 2, inset). In the latter orientation, magnetization isotherms approach saturation significantly faster, suggesting that the normal to the pellet faces is an easier magnetic direction. The demagnetization factor has been neglected here because of the relatively low magnetic density of the material and the magnetic field employed. Its contribution is however expected to be opposite to the observed trend.

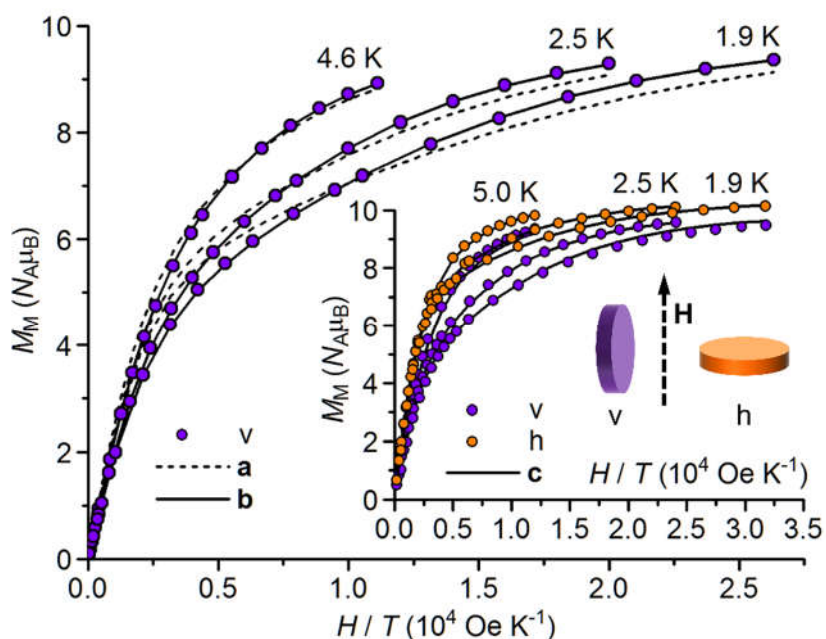


Fig. 2. Isothermal M_M vs. H/T curves recorded after rough crushing and pelletization of the sample. The inset shows angle-resolved measurements up to 60 kOe on the same pellet and the definition of pellet orientation in applied field \mathbf{H} : v = vertical. h = horizontal. The dashed and solid curves provide the best fit with the parameters reported in entries **a-c** of Table 1. (For interpretation of the references to color in this figure legend, the reader is referred to the web version of this article.)

Table 1. Best-fit parameters over the data in Fig. 2, with g fixed at 2.00 throughout

entry	orientation ^a	D (cm ⁻¹)	$a_2(v)$	$a_2(h)$	S ($N_A\mu_B$) ^b
a	v	-0.511(14)	-	-	0.257
b	v	-0.4145(12)	-0.0986(11)	-	0.0197
c	v, h ^c	-0.390(5)	-0.068(4)	0.165(4)	0.0867
d	v	-0.4142(15)	-	-	0.0313

^a pellet orientation, as defined in Fig. 2 (inset); ^b standard error of the regression; ^c calculated data for horizontal pellet orientation were multiplied by an adjustable scale factor to account for the enhanced inductive coupling with the pickup coils [best fit value = 1.050(2)].

While the detailed angular-dependent response of the pellet would be easy to determine, we have not pursued this task. Rather, we show here that preferential orientation can be efficiently accounted for by refining a single LS parameter, which describes the leading part of a non-spherical distribution.

We work in the molecular reference frame xyz (where z is the magnetic easy axis) and apply the magnetic field \mathbf{H} at polar angles θ and ϕ . If $M(H, \theta, \phi, T)$ with $H = |\mathbf{H}|$ is the molecular magnetization in the direction of the applied field, the average magnetization is obtained by integrating over all accessible θ and ϕ values, namely:

$$\bar{M}(H, T) = \int_0^{2\pi} \int_0^\pi \rho(\theta, \phi) M(H, T, \theta, \phi) \sin\theta d\theta d\phi = \sum_{kq} b_{kq} m_{kq}(H, T) \quad (3)$$

The distribution function $\rho(\theta, \phi)$ accounts for the probability of finding the magnetic field at polar angles θ and ϕ in the molecular reference frame. It is assumed to be field and temperature independent, meaning that the crystallites must be properly restrained to avoid field-induced alignment during measurements. In Eq. (3), b_{kq} and $m_{kq}(H, T)$ are the expansion coefficients of $\rho(\theta, \phi)$ and $M(H, T, \theta, \phi)$, respectively, in series of real spherical harmonics $Y_{kq}(\theta, \phi)$. Because magnetic properties are invariant upon inversion of magnetic field, the summation contains only even-order (k) terms. In absence of preferential orientation, the distribution function is angle independent and normalization condition requires $\rho(\theta, \phi) = (4\pi)^{-1}$. When the magnetic response at the molecular level is independent of ϕ , Eq. (3) contains only terms with cylindrical symmetry around z , i.e. $q = 0$. This condition is largely met in Fe₄ complexes, which have quasi-axial symmetry, and in most SMMs. Following the notation in Ref. [15], the true distribution function can then be replaced by a ϕ -independent effective one:

$$\rho_{\text{eff}}(\theta) = \sum_k \frac{1}{2} a_k P_k(\cos\theta) \quad (4)$$

where $P_k(\cos\theta)$ are Legendre polynomials of even order. Retaining only terms with $k = 0$ and 2 gives

$$\rho_{\text{eff}}(\theta) = \frac{a_0}{2} + \frac{a_2}{4} (3\cos^2\theta - 1) \quad (5)$$

where $a_0 = (2\pi)^{-1}$ ensures normalization. Eq. (3) can be rewritten as:

$$\bar{M}(H, T) = \frac{1}{2} \int_0^\pi [1 + \pi a_2 (3\cos^2\theta - 1)] M(H, T, \theta) \sin\theta d\theta \quad (6)$$

The impact of a_2 on magnetization curves is shown in Fig. 3 for representative **temperature** and D values. Preferential orientation primarily changes the low-field portion of the curves: positive (negative) a_2 values result in higher (lower) slope (i.e. low-field susceptibility), as expected for a prolate (oblate) effective distribution along z . Positive (negative) a_2 values also yield a more (less) rapid approach to saturation. However, since for isotropic g the saturation magnetization is orientation-independent ($N_A \mu_B g S$), the high-field magnetic behavior is much less sensitive to preferential orientation. Obviously, for a given distribution function $\rho(\theta, \phi)$, the value of a_2 depends on how the distribution is probed, that is, on sample orientation. For instance, if the actual distribution is axial along the cylindrical axis of the pellet, the rotation properties of spherical harmonic Y_{20} [29] yield the relationship $a_2(v) = -(1/2)a_2(h)$; if the actual distribution has its axis in the plane of the pellet, then $a_2(v)$ may span the interval between $-2a_2(h)$ and $a_2(h)$, depending on the orientation of the magnetic field in the pellet's plane.

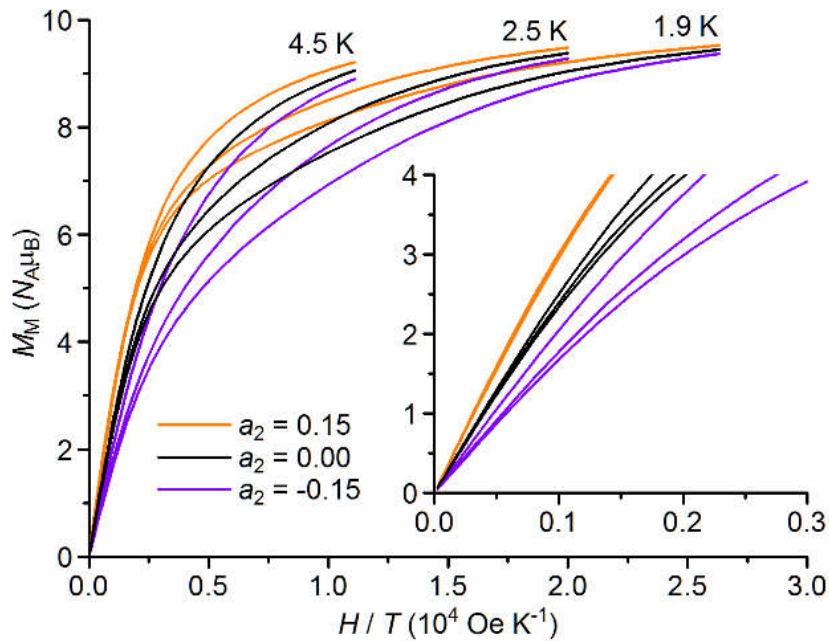


Fig. 3. Isothermal M_M vs. H/T curves at 4.5, 2.5 and 1.9 K calculated for $D = -0.40 \text{ cm}^{-1}$, $g = 2.00$ and different values of preferential orientation a_2 parameter. The inset shows a magnified view of the low-field portion of the graph. (For interpretation of the references to color in this figure legend, the reader is referred to the web version of this article.)

Introducing a_2 as an adjustable parameter yields a vastly improved fit to magnetization data in the main panel of Fig. 2, with a 13-fold decreased standard error of the regression (entry **b** in Table 1). The negative $a_2(v)$ leads to a lower initial slope of M_M vs. H curves with respect to a true powder average, thereby explaining the unusually low $\chi_M T$ product measured at low T (Fig. 1). In this orientation of the pellet, then, the probability of finding the applied field orthogonal to the easy axis is larger than for a randomly oriented sample. The angle-dependent curves reported in the inset of Fig. 2 were also simultaneously fitted with a common D parameter but independent $a_2(v)$ and $a_2(h)$ values. The fit afforded the parameters listed as entry **c** in Table 1. The slightly different $a_2(v)$ with respect to entry **b** may reflect a different orientation of \mathbf{H} in the plane of the pellet (a parameter that was not experimentally controlled). More important, $a_2(h)$ is now positive, indicating that small θ values are more represented than in a spherical distribution. The fact that $a_2(h)$ is about twice as large as $|a_2(v)|$ is reminiscent of the rotation properties of spherical harmonic Y_{20} [29] and suggests that the distribution of molecular easy axes is biased towards the cylindrical axis of the pellet.

The sample was finally subject to thorough grinding, pelletized again and inserted vertically in a SQUID magnetometer. As expected, the low-field $\chi_M T$ product remains higher at low T (black circles in Fig. 1) and the whole curve can be accurately fitted with $g = 1.9922(10)$, $J = 16.04(5) \text{ cm}^{-1}$, $J' = 0.07(3) \text{ cm}^{-1}$ and $B_2^0 = -0.218(6) \text{ cm}^{-1}$. The calculated D value for the ground manifold ($-0.450(19) \text{ cm}^{-1}$) is now in the typical range for Fe_4 complexes [19]. The three M_M vs. H datasets collected on this new sample can be well fitted omitting preferential orientation (entry **d** in Table 1 and Fig. S1). Comparison of entries **b** and **d**, which are based on data recorded with the same instrument and sample arrangement, is particularly meaningful. It shows that application of our correction scheme to a dataset affected by preferential orientation gives the same D parameter (**b**) as the analysis of a true powder average (**d**). The accuracy of the spin-Hamiltonian parameters so-obtained was finally evaluated from high frequency EPR spectra recorded at 190 and 230 GHz at low temperature (Fig. S2). Use of the Hamiltonian:

$$\hat{H}_{\text{EPR}} = \mu_{\text{B}} \hat{\mathbf{S}} \cdot \bar{\mathbf{g}} \cdot \mathbf{B} + D[\hat{S}_z^2 - S(S+1)/3] + E(\hat{S}_x^2 - \hat{S}_y^2) + B_4^0 \hat{O}_4^0 \quad (7)$$

where $\hat{O}_4^0 = 35\hat{S}_z^4 - [30S(S+1) - 25]\hat{S}_z^2 - 6S(S+1) + 3S^2(S+1)^2$ [28], afforded $D = -0.430(1) \text{ cm}^{-1}$, $E = 0.035(3) \text{ cm}^{-1}$, $B_4^0 = 1.2(1) \cdot 10^{-5} \text{ cm}^{-1}$, and $g_x = g_y = 1.995(10)$, $g_z = 2.002(5)$.

4. Conclusions

Although preferential orientation can be avoided by suitable sample preparation, producing a better sample might be impossible or inconvenient. In such cases, a simple one-parameter correction can be introduced to extract the relevant information on magnetic anisotropy (i.e. D value), with a vastly improved quality of fit. The method is best applied to the analysis of isothermal M vs. H curves and does not introduce any significant loss in accuracy as compared with re-grinding and re-measuring. Its applicability is however not limited to the determination of D in systems with a well-isolated ground spin state, but can be extended to all molecular materials with a predominantly axial magnetic response, including monolanthanoid complexes currently investigated as high-performance SMMs [3–5].

Declaration of Competing Interest

There is no conflict of interest.

Author Contributions

Andrea Cornia: Conceptualization, Methodology, Software, Formal Analysis, Writing - Original Draft, Supervision; **Anne-Laure Barra**: Formal Analysis, Investigation, Writing - Review & Editing; **Giordano Poneti**: Investigation, Writing - Review & Editing; **Erik Tancini**: Resources, Writing - Review & Editing; **Roberta Sessoli**: Investigation, Writing - Review & Editing.

Acknowledgements

This work was supported by Italian MIUR (FIRB project RBAP117RWN). We thank R. Clérac (Univ. Bordeaux & CNRS, France) and R. Boča (Slovak University of Technology, Bratislava, Slovakia) for advice and helpful discussion.

References

- [1] A. Caneschi, D. Gatteschi, R. Sessoli, A.L. Barra, L.C. Brunel, M. Guillot, Alternating current susceptibility, high field magnetization, and millimeter band EPR evidence for a ground $S = 10$ state in $[\text{Mn}_{12}\text{O}_{12}(\text{CH}_3\text{COO})_{16}(\text{H}_2\text{O})_4] \cdot 2\text{CH}_3\text{COOH} \cdot 4\text{H}_2\text{O}$, *J. Am. Chem. Soc.* 113 (1991) 5873–5874. <https://doi.org/10.1021/ja00015a057>.
- [2] R. Sessoli, D. Gatteschi, A. Caneschi, M.A. Novak, Magnetic bistability in a metal-ion cluster, *Nature*. 365 (1993) 141–143. <https://doi.org/10.1038/365141a0>.
- [3] F.-S. Guo, B.M. Day, Y.-C. Chen, M.-L. Tong, A. Mansikkamäki, R.A. Layfield, Magnetic hysteresis up to 80 kelvin in a dysprosium metallocene single-molecule magnet, *Science* (80-.). 362 (2018) 1400–1403. <https://doi.org/10.1126/science.aav0652>.
- [4] C.A.P. Goodwin, F. Ortu, D. Reta, N.F. Chilton, D.P. Mills, Molecular magnetic hysteresis at 60 kelvin in dysprosocenium, *Nature*. 548 (2017) 439–442. <https://doi.org/10.1038/nature23447>.
- [5] F.-S. Guo, B.M. Day, Y.-C. Chen, M.-L. Tong, A. Mansikkamäki, R.A. Layfield, A Dysprosium Metallocene Single-Molecule Magnet Functioning at the Axial Limit, *Angew. Chem. Int. Ed.* 56 (2017) 11445–11449. <https://doi.org/10.1002/anie.201705426>.
- [6] R. Sessoli, Magnetic molecules back in the race, *Nature*. 548 (2017) 400–401. <https://doi.org/10.1038/548400a>.
- [7] K.L.M. Harriman, D. Errulat, M. Murugesu, Magnetic Axiality: Design Principles from Molecules to Materials, *Trends Chem.* 1 (2019) 425–439. <https://doi.org/10.1016/j.trechm.2019.04.005>.
- [8] R. Boča, *Theoretical Foundations of Molecular Magnetism*, Elsevier Science, Amsterdam, 1999.
- [9] N.F. Chilton, R.P. Anderson, L.D. Turner, A. Soncini, K.S. Murray, PHI: A powerful new program for the analysis of anisotropic monomeric and exchange-coupled polynuclear d- and f-block complexes, *J. Comput. Chem.* 34 (2013) 1164–1175. <https://doi.org/10.1002/jcc.23234>.
- [10] M. Edén, M.H. Levitt, Computation of Orientational Averages in Solid-State NMR by Gaussian Spherical Quadrature, *J. Magn. Reson.* 132 (1998) 220–239. <https://doi.org/10.1006/jmre.1998.1427>.
- [11] B. Stevansson, M. Edén, Efficient orientational averaging by the extension of Lebedev grids via regularized octahedral symmetry expansion, *J. Magn. Reson.* 181 (2006) 162–176. <https://doi.org/10.1016/j.jmr.2006.04.008>.
- [12] A. Ponti, Simulation of Magnetic Resonance Static Powder Lineshapes: A Quantitative Assessment of Spherical Codes, *J. Magn. Reson.* 138 (1999) 288–297. <https://doi.org/10.1006/jmre.1999.1758>.
- [13] A. Cornia, A.-L. Barra, V. Bulicanu, R. Clérac, M. Cortijo, E.A. Hillard, R. Galavotti, A. Lunghi, A. Nicolini, M. Rouzières, L. Sorace, F. Totti, The Origin of Magnetic Anisotropy and Single-Molecule Magnet Behavior in Chromium(II)-Based Extended Metal Atom Chains, *Inorg. Chem.* 59 (2020) 1763–1777. <https://doi.org/10.1021/acs.inorgchem.9b02994>.
- [14] U.F. Kocks, C.N. Tomé, H.-R. Wenk, *Texture and Anisotropy. Preferred Orientations in Polycrystals and their Effect on Materials Properties*, Cambridge University Press, Cambridge, UK, 1998.

- [15] N.A. Chumakova, T.S. Yankova, A.K. Vorobiev, EPR Study of the Orientation Distribution Function of HO₂• Radicals Ordered by Light Irradiation, *Appl. Magn. Reson.* 33 (2008) 117–126. <https://doi.org/10.1007/s00723-008-0047-2>.
- [16] S. Stoll, CW-EPR Spectral Simulations, *Methods Enzymol.* 563 (2015) 121–142. <https://doi.org/10.1016/bs.mie.2015.06.003>.
- [17] P.S. Whitfield, Spherical harmonics preferential orientation corrections and structure solution from powder diffraction data – a possible avenue of last resort, *J. Appl. Crystallogr.* 42 (2009) 134–136. <https://doi.org/10.1107/S0021889808041149>.
- [18] J.-P. Kappler, E. Otero, W. Li, L. Joly, G. Schmerber, B. Muller, F. Scheurer, F. Leduc, B. Gobaut, L. Poggini, G. Serrano, F. Choueikani, E. Lhotel, A. Cornia, R. Sessoli, M. Mannini, M.-A. Arrio, P. Sainctavit, P. Ohresser, Ultralow-temperature device dedicated to soft X-ray magnetic circular dichroism experiments, *J. Synchrotron Radiat.* 25 (2018) 1727–1735. <https://doi.org/10.1107/S1600577518012717>.
- [19] A. Cornia, M. Mannini, R. Sessoli, D. Gatteschi, Propeller-Shaped Fe₄ and Fe₃M Molecular Nanomagnets: A Journey from Crystals to Addressable Single Molecules, *Eur. J. Inorg. Chem.* 2019 (2019) 552–568. <https://doi.org/10.1002/ejic.201801266>.
- [20] S. Accorsi, A.-L. Barra, A. Caneschi, G. Chastanet, A. Cornia, A.C. Fabretti, D. Gatteschi, C. Mortalò, E. Olivieri, F. Parenti, P. Rosa, R. Sessoli, L. Sorace, W. Wernsdorfer, L. Zobbi, Tuning anisotropy barriers in a family of tetrairon(III) single-molecule magnets with an S = 5 ground state, *J. Am. Chem. Soc.* 128 (2006) 4742–4755. <https://doi.org/10.1021/ja0576381>.
- [21] E. Tancini, M. Mannini, P. Sainctavit, E. Otero, R. Sessoli, A. Cornia, On-Surface Magnetometry: The Evaluation of Superexchange Coupling Constants in Surface-Wired Single-Molecule Magnets, *Chem. Eur. J.* 19 (2013) 16902–16905. <https://doi.org/10.1002/chem.201303585>.
- [22] L. Gregoli, C. Danieli, A.-L. Barra, P. Neugebauer, G. Pellegrino, G. Poneti, R. Sessoli, A. Cornia, Magnetostructural correlations in tetrairon(III) single-molecule magnets, *Chem. Eur. J.* 15 (2009) 6456–6467. <https://doi.org/10.1002/chem.200900483>.
- [23] G.A. Bain, J.F. Berry, Diamagnetic Corrections and Pascal's Constants, *J. Chem. Educ.* 85 (2008) 532–536. <https://doi.org/10.1021/ed085p532>.
- [24] E04FCF, E04YCF and F02ABF, NAG Fortran Library Routines (Mark 17), NAG Ltd, Oxford, UK, 1996.
- [25] S. Mossin, H. Weihe, A.-L. Barra, Is the Axial Zero-Field Splitting Parameter of Tetragonally Elongated High-Spin Manganese(III) Complexes Always Negative?, *J. Am. Chem. Soc.* 124 (2002) 8764–8765. <https://doi.org/10.1021/ja012574p>.
- [26] C.J.H. Jacobsen, E. Pedersen, J. Villadsen, H. Weihe, ESR characterization of trans-VII(py)₄X₂ and trans-MnII(py)₄X₂ (X = NCS, Cl, Br, I; py = pyridine), *Inorg. Chem.* 32 (1993) 1216–1221. <https://doi.org/10.1021/ic00059a031>.
- [27] L. Vergnani, A.-L. Barra, P. Neugebauer, M.J. Rodriguez-Douton, R. Sessoli, L. Sorace, W. Wernsdorfer, A. Cornia, Magnetic Bistability of Isolated Giant-Spin Centers in a Diamagnetic Crystalline Matrix, *Chem. Eur. J.* 18 (2012) 3390–3398. <https://doi.org/10.1002/chem.201103251>.
- [28] A. Abragam, B. Bleaney, *Electron paramagnetic resonance of transition ions*, Oxford University Press, Oxford, UK, 2012.
- [29] J. Ivanic, K. Ruedenberg, Rotation Matrices for Real Spherical Harmonics. Direct Determination by Recursion, *J. Phys. Chem.* 100 (1996) 6342–6347. <https://doi.org/10.1021/jp953350u>.